Carbohydrate Polymers 88 (2012) 1387–1394

Contents lists available at SciVerse ScienceDirect

Carbohydrate Polymers

journal homepage: www.elsevier.com/locate/carbpol

Cyclodextrin nanosponges as novel green flame retardants for PP, LLDPE and PA6

Jenny Alongi[a,*], Merima Poskovic[a], Visakh P.M.[b], Alberto Frache[a], Giulio Malucelli[a]

[a] Dipartimento di Scienza dei Materiali e Ingegneria Chimica, Politecnico di Torino, sede di Alessandria, Viale Teresa Michel 5, 15121 Alessandria, Italy
[b] School of Chemical Sciences, Mahatma Gandhi University, Kottayam 686560, Kerala, India

ARTICLE INFO

Article history:
Received 21 December 2011
Received in revised form 30 January 2012
Accepted 13 February 2012
Available online 28 February 2012

Keywords:
β-Cyclodextrins
Nanosponges
Flame retardants
Polyolefins
Polyamide 6
Cone calorimetry

ABSTRACT

Novel green flame retardant systems based on a complex of cyclodextrin nanosponges and phosphorus derivatives (namely, triethylphosphate and ammonium polyphosphate) have been prepared. The above additives have been subsequently melt compounded with polypropylene, linear low density polyethylene or polyamide 6 in order to improve the thermal stability of the latter polymers and their flame retardancy properties (assessed by combustion and flammability tests). The role of cyclodextrin nanosponges both as a carbon source and a foaming agent in such intumescent formulations has been demonstrated: indeed, the phosphorus derivatives are embedded and protected by the nanosponge architectures and thus are able to generate phosphoric acid directly *in situ* at high temperatures. As a consequence, cyclodextrin nanosponges dehydrate in presence of this acid source, giving rise to water vapour, favouring char formation and thus significantly enhancing the polymer resistance toward combustion.

1. Introduction

Intumescent technology has found a place in polymer science as an efficient method for providing flame retardancy properties to polymer formulations in a safer way with respect to halogens and halogen derivatives (Bourbigot & Duquesne, 2010; Bourbigot, Le Bras, Duquesne, & Rochery, 2004; Duquesne, Magnet, Jama, & Delobel, 2005; Duquesne et al., 2009; Le Bras, Camino, Bourbigot, & Delobel, 1998; Morgan & Wilkie, 2007). When an intumescent material is subjected to a heat flow, it develops a carbonaceous shield on its surface, commonly called char. This protection acts as a physical barrier able to limit the heat, fuel and oxygen transfer between the flame and polymer. Usually, the intumescent material consists of three components:

- an acid source (i.e. ammonium phosphates or polyphosphates), which releases phosphoric acid at ca. 150 °C,
- a carbon source (pentaerythritol, arabitol, sorbitol, inositol, saccharides, polysaccharides, etc.),
- a blowing agent (guanidine, melamine, etc.), which releases great amounts of expandable or non-combustible gases (ammonia or carbon dioxide) upon heating.

The char is the result of a sequence of reactions, occurring in between the three components of the intumescent formulation. Some species, such as ammonium phosphates or polyphosphates, possess a great advantage in comparison with other chemicals for an industrial application, since they can act as both the acid source and the blowing agent (ammonia release), at the same time.

However, the intumescent concept requires a loading factor up to 30% by weight, which determines a significant worsening of the compound mechanical properties and does not allow to consistently reach a fire resistance level comparable with that derived from the use of halogens.

In order to increase the efficiency of intumescent systems or to reduce the flame retardant content without significantly changing their fire performance, synergistic effects have been explored. In particular, some efforts have been carried out using nanoarchitectures, such as nanoparticles (Bourbigot et al., 2004; Duquesne et al., 2005) or cyclodextrins (Feng, Su, & Zhu, 2011; Hashidzume, Tomatsu, & Harada, 2006; Huang, Allen, & Tonelli, 1999; Huang, Gerber, Lu, & Tonelli, 2001; Le Bras, Bourbigot, Le Tallec, & Laureyns, 1997; Wang & Li, 2010). These latter species show a double advantage due to both the nanosized and polysaccharide nature (i.e. they involve *green* chemistry, starting from natural starch derivatives). Recently, we have demonstrated that cyclodextrin nanosponges (NS) can be used in combination with phosphorus molecules in order to enhance the thermal stability of an ethylene-vinyl-acetate copolymer (Alongi, Poskovic, Frache, & Trotta, 2010) and polyamide 6,6 (Enescu, Alongi, & Frache, 2012). They show a porous morphology, a limited toxicity, outstanding stability (up to ca. 300 °C in air)

* Corresponding author. Tel.: +39 0131 229337; fax: +39 0131 229399.
E-mail address: jenny.alongi@polito.it (J. Alongi).

0144-8617/$ – see front matter © 2012 Elsevier Ltd. All rights reserved.
doi:10.1016/j.carbpol.2012.02.038

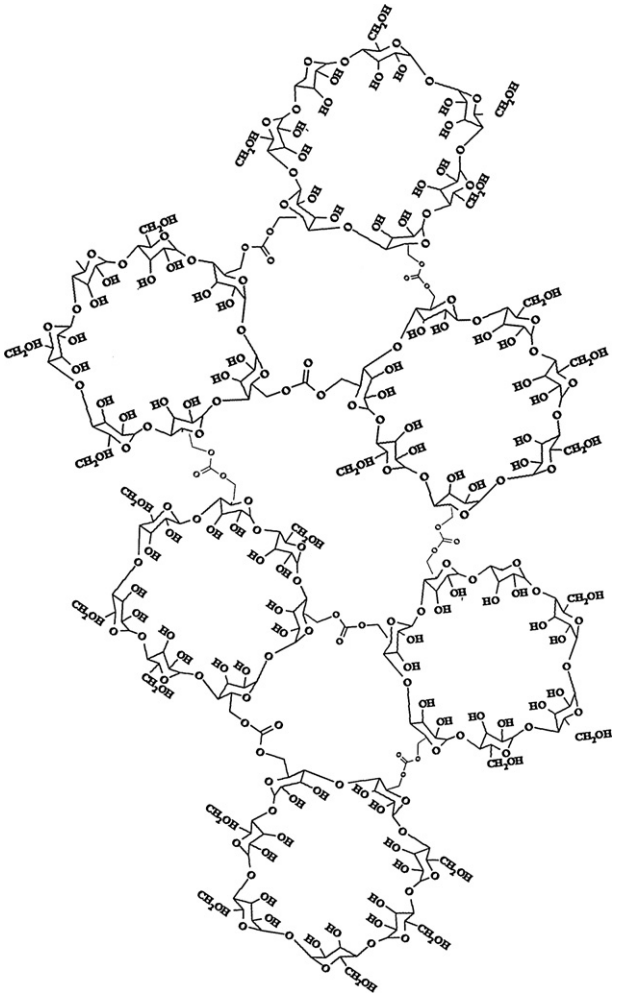

Fig. 1. Chemical structure of β-cyclodextrin nanosponges.

and are able to capture, transport and selectively deliver a huge variety of substances because of their tuneable polarity and their 3D structure containing nanocavities.

The nanosponges employed in the present study have been synthesized from β-cyclodextrins (which are cyclic oligosaccharides formed by 6–8 glucose molecules bonded with α-1,4-glycosidic bonds, having a characteristic truncated cone structure) crosslinked by organic carbonates. The resulting network is characterized by both internal and external cavities, as shown in Fig. 1, where phosphorus species can be easily entrapped. As a consequence, such structure should be able to finely tune the flame retardant release upon heating, thus enhancing the fire resistance and the overall combustion behaviour of the polymer matrix, which nanosponges have been previously compounded with.

Therefore, the present paper aims to assess the use of cyclodextrin nanosponges in combination with phosphorus derivatives, as green flame retardant systems for polyolefins (namely, polypropylene and linear low density polyethylene) and polyamide 6, optimizing a formulation in which the saccharide represents the main component, while the content of phosphorus derivatives is significantly lowered with respect to the current industrial formulations of flame retardants. To this aim, the thermal and thermo-oxidative stability of such formulations have been assessed. Furthermore, their flammability and combustion behaviour have been investigated through vertical flame tests and cone calorimetry, respectively.

Table 1
Composition of the melt compounded systems.

Sample	NS content [wt.%]	TEP content [wt.%]	APP content [wt.%]
PP-NS	10		
PP-NSTEP	7	3	–
PP-NSTEP*	10	5	–
PP-NSAPP	7.5	–	7.5
LLDPE-NS	10	–	–
LLDPE-NSTEP	7	3	–
LLDPE-NSTEP*	10	5	–
LLDPE-NSAPP	7.5	–	7.5
PA6-NS	10	–	–
PA6-NSTEP	7	3	–
PA6-NSTEP*	10	5	–

The great advantage of such novel green flame retardants is that nanosponges can act as both a carbon source and a foaming agent in an intumescent formulation. At the same time, the particular nanosponge architecture embeds and protects the phosphorus molecules, thus allowing to directly generate phosphoric acid *in situ*. The latter species favour the nanosponge dehydration, giving rise to water vapour and consequently inducing char formation.

2. Experimental

2.1. Materials

Polypropylene (PP, HP500N, density: 0.9 g/cm^3; MFI at 230 °C/2.16 kg: 12 g/10 min) and linear low-density polyethylene (LLDPE, Lupolex 18QFA, density: 0.9 g/cm^3; MFI at 230 °C/2.16 kg: 12 g/10 min) were purchased by Basell Polyolefins S.r.l. (Ferrara, Italy). Polyamide 6 (PA6, Aquamid AQ27000, density: 1.14 g/cm^3) was kindly supplied by Aquafil S.p.A. (Trento, Italy).

Cyclodextrin nanosponges were synthesized following the detailed procedure described elsewhere (Alongi et al., 2010). Their chemical structure is given in Fig. 1. Triethylphosphate (TEP) and ammonium polyphosphate (APP), both reagent grades, were purchased from Sigma Aldrich, Inc. and Clariant, Inc., respectively, and used as received. As far as polyamide 6 is concerned, only TEP was used since APP decomposes at the compounding temperature, thus inducing polymer degradation.

2.2. Compounding of NS-phosphorus derivative complexes with PP, LLDPE and PA6

Different complexes of NS-phosphorus derivatives were prepared through a simple mechanical grinding. Then they were compounded with PP, LLDPE or PA6, using an internal mixer (Brabender W50E model, 40 rpm for 3 min) at 190, 120 and 240 °C, respectively. The compositions of the compounds are listed in Table 1, where NSTEP and NSTEP* have a different content of that phosphorus derivative.

2.3. Characterization

The thermal properties of the investigated formulations were evaluated by thermogravimetry (TG) and differential scanning calorimetry (DSC). TG analyses were performed by heating ca. 10 mg samples in alumina pans from 50 to 800 °C with a heating rate of 10 °C/min, under nitrogen or air atmosphere, using a TAQ 500 analyser. DSC analyses were carried out using a QA1000TA apparatus. Three consecutive scans were performed according to the following scheme:

1st scan: heating up from 25 to 280 °C at 20 °C/min, isothermal step at 280 °C for 5 min.
2nd scan: cooling down from 280 to 25 °C at 10 °C/min, isothermal step at 25 °C for 5 min.
3rd scan: same as 1st scan.

The degree of crystallinity (X_c) was calculated according to the method proposed by Tjong & Bao (2004). Therefore:

$$\text{for pure polymers}: X_c = \frac{\Delta H_c}{\Delta H_{m0}} \times 100 \quad (1)$$

$$\text{for melt compounds}: X_c = \frac{\Delta H_c}{\Delta H_{m0}} \times 100(1 - \Phi) \quad (2)$$

where ΔH_{m0} is the theoretical enthalpy of fusion of the 100% crystalline polymers (178, 140 and 230 J/g for PP, LLDPE and PA6, respectively), ΔH_c is the experimental crystallization enthalpy and Φ is the content of nanosponge complex compounded with the different polymer matrices (0.10 and 0.15, Table 1).

In order to describe a realistic fire scenario, it is important to test both the ignitability of a sample in presence of a flame spread (flammability) and the combustion behaviour of the same sample under the irradiative heat flow developed as a consequence of the flame exposure. Therefore, the flame retardancy properties of the prepared samples were measured according to two different tests.

The combustion behaviour was determined by cone calorimetry. The tests were carried out using a cone calorimeter (Fire Testing Technology, FTT) according to the ISO5660 standard. Square specimens (50 mm × 50 mm × 3 mm) were irradiated at 35 kW/m^2 in horizontal configuration. The specimens were placed in a sample holder and maintained in the correct configuration by a metallic grid. Time To Ignition (TTI, s), Total Heat Release (THR, kW/m^2), Heat Release Rate (HRR, kW/m^2) and its peak (pkHRR, kW/m^2), Effective Heat of Combustion (EHC, MJ/kg) and Mass Loss Rate (MLR, g/s) were measured. Total Smoke Release (TSR, m^2/m^2), Specific Extinction Area (SEA, m^2/kg) and Smoke Production Rate (SPR, m^2/s) were evaluated, as well. For each sample, the experiments were repeated three times in order to ensure reproducible and significant data. The experimental error was within 5%.

The flammability tests in vertical configuration were carried out by applying a methane flame for 10 s at the bottom of the specimen (127 mm × 127 mm × 3.2 mm) and repeating the application at least two times.

3. Results and discussion

3.1. Thermal stability

As mentioned in Section 2, the thermal and thermo-oxidative stability of the nanosponge-based compounds have been assessed by thermogravimetric analyses in nitrogen and air, respectively.

Fig. 2a–c plots the weight loss and its corresponding rate in nitrogen as a function of temperature for PP, LLDPE and PA6 systems, respectively; Table 2 summarizes the collected data.

First of all, it is noteworthy that the presence of NS strongly affects the weight loss at low temperatures, as shown by the decrease of $T_{onset10\%}$ values (Table 2) and well depicted in Fig. 2a–c. This anticipation can be probably ascribed to the presence of hydroxyl groups in the cyclodextrin units that catalyse the decomposition of PP, LLDPE and PA6, as already described in the literature as far as the catalytic effect of nanoparticles bearing hydroxyl groups is concerned (Xie et al., 2001). Referring to the investigated polyolefins, this detrimental effect can be partially overcome in

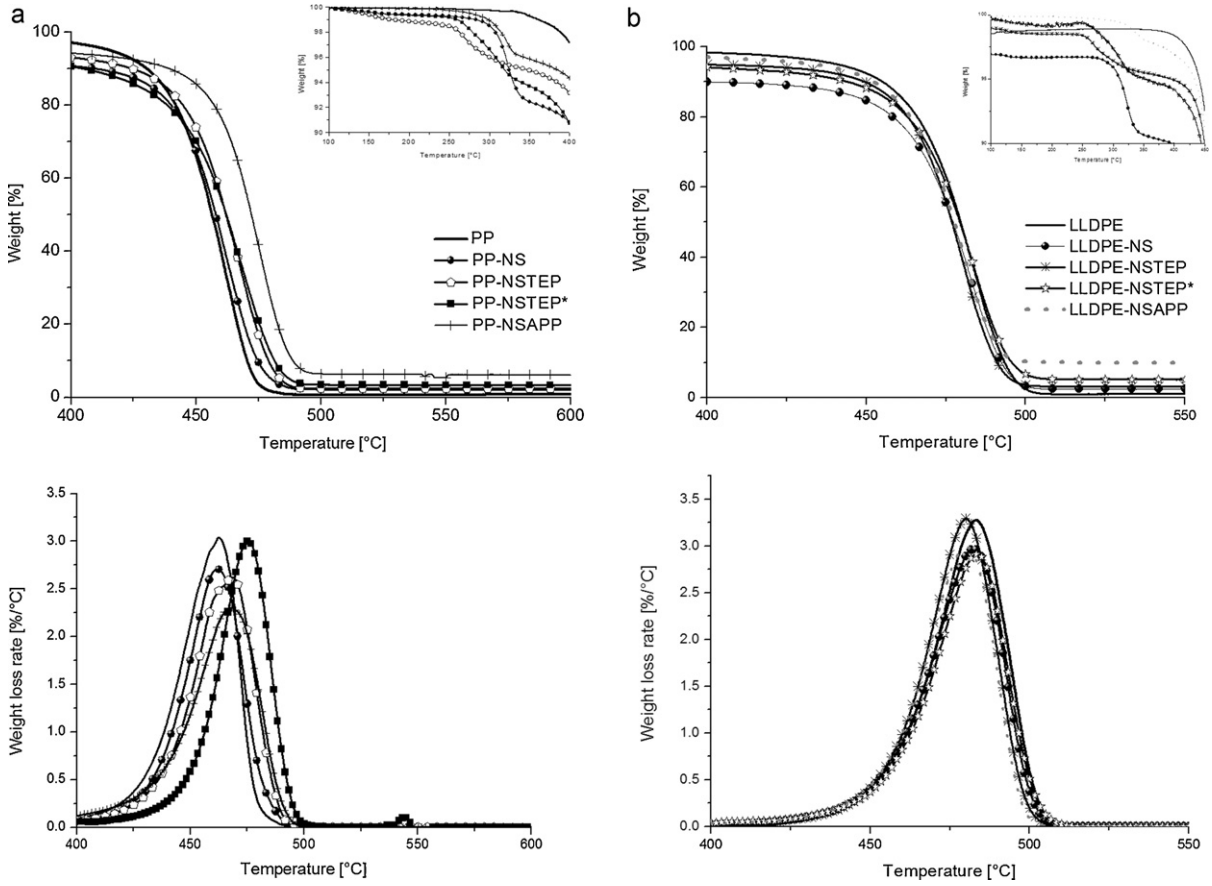

Fig. 2. TG and dTG curves of PP (a), LLDPE (b) and PA6 (c) systems in nitrogen.

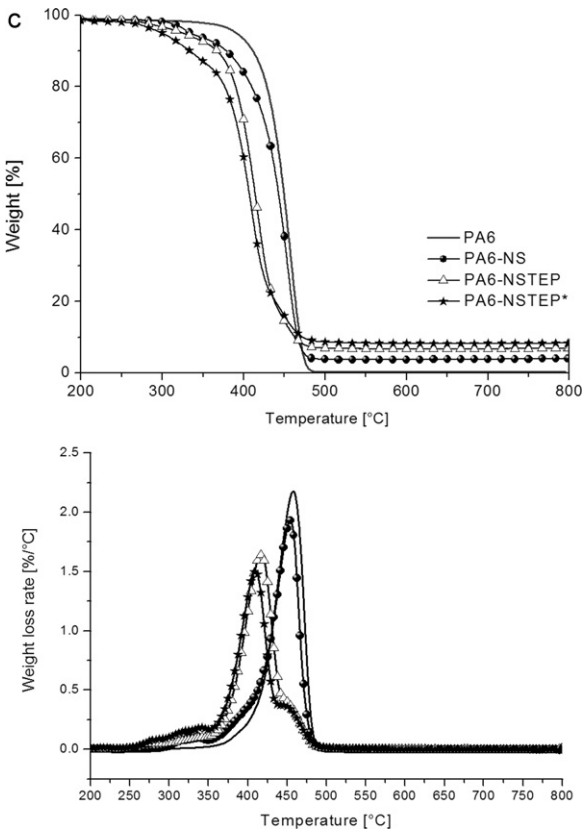

Fig. 2. (*continued*).

the presence of NS-phosphorus derivatives, as clearly indicated in Table 2 by the increase of $T_{onset10\%}$ values (compare PP- or LLDPE-NS *vs.* PP- or LLDPE-NSTEP, NSTEP* and NSAPP): a possible explanation of this behaviour relates to the capability of such complexes to interfere with the polymer degradation mechanism through a competitive way. Indeed, the phosphorus derivatives are able to generate phosphoric acid directly *in situ* during the heating up of the compounds: as a consequence, cyclodextrin nanosponges dehydrate in presence of this acid source, giving rise to water vapour, favouring the char formation and thus significantly enhancing the thermal stability of the polyolefins. Furthermore, it is noteworthy that this behaviour is not observed in the case of PA6, because this polymer already tends to form char residue, as clearly described in the literature (Riva, Camino, Fomperiere, & Amigouet, 2003).

In addition, the degradation profiles of PP, LLDPE and PA6 do not change in a significant way in the presence of NS or NS-phosphorus complexes, regardless of the flame retardant content (namely 10 or 15 wt.%, Fig. 2a and b). Polyolefins-based compounds do not exhibit a significant variation of their T_{max} values (i.e. temperatures, at which the maximum weight loss occurs, see Table 2), whereas these values are drastically reduced for PA6-based compounds. This latter behaviour can be ascribed to the presence of TEP, which anticipates the weight loss of the polymer, as already observed for polar systems such as polyurethane foams (Lorenzetti, Modesti, Besco, Hrelja, & Donadi, 2011) or an ethylene-vinyl-acetate copolymer (Alongi et al., 2010).

The presence of both NS and NS complexes turns out to promote the residue formation at 700 °C for all the polymers investigated, as clearly indicated in the last column of Table 2. In particular, this effect is very significant for PP compounded with NS (Fig. 2a and Table 2): this behaviour can be ascribed to the action of NS alone or a joint effect between NS and phosphorus derivatives that favour the formation of a carbonaceous multilamellar structure (char), stable at high temperatures. Indeed, such char is able to limit the production of volatile species induced by PP degradation and favour its carbonization, so that the formation of a high residue at 700 °C is promoted. Comparing the thermal performances of PP-NSTEP and PP-NSTEP* systems, it is worthy to note that the thermal stability of PP in nitrogen does not increase in a remarkable way when the flame retardant content is increased from 10 to 15 wt.%. The most interesting result for PP has been observed using the NS-APP complex, since $T_{onset10\%}$ and T_{max1} were found higher with respect to pure PP (439 and 476 *vs.* 430 and 463 °C) as well as higher are the residues left both at T_{max1} and 700 °C (71.9 and 6.0 *vs.* 34.4 and 0.5%).

Comparing the residues at T_{max1} and 700 °C collected in Table 2 and plotted in Fig. 2a and b, it is worthy to note that LLDPE performances in the presence of NS complexes are lower than those of PP-based counterparts, which substantially show higher residues, being equal the type and content of NS-phosphorus complex. Finally, PA6 (Fig. 2c) shows the occurrence of a joint effect between NS and phosphorus derivatives, which pushes the residue formation up to 6.8 and 8.6% in the case of PA6-NSTEP and PA6-NSTEP*, respectively.

The investigation of the thermo-oxidative stability of the prepared compounds puts in evidence the anticipation of the degradation in air, regardless of the polymer matrix and flame retardant formulation employed (Fig. 3a–c and Table 3), with the only exception of LLDPE added with NS-APP complex (Fig. 3b, broken line). In detail, PP degrades by two decomposition steps at 323 and 480 °C (Fig. 3a and Table 3). The first peak is affected only by the presence of TEP. T_{max1} values for PP-NSTEP and PP-NSTEP* are lower

Table 2
Thermogravimetric analyses in nitrogen.

Sample	$T_{onset10\%}$ [°C]	T_{max} [a] [°C]	Residue at T_{max1} [b] [%]	Residue at 700 °C [%]
PP	430	463	34.4	0.5
PP-NS	406	462	37.7	2
PP-NSTEP	424	469	47.0	2.6
PP-NSTEP*	420	468	47.8	3.0
PP-NSAPP	439	476	71.9	6.0
LLDPE	457	483	40.3	<1
LLDPE-NS	437	483	32.7	2.5
LLDPE-NSTEP	451	480	30.7	3.3
LLDPE-NSTEP*	450	478	28.0	2.9
LLDPE-NSAPP	452	480	33.3	3.0
PA6	411	458	32.3	<0.5
PA6-NS	379	455	9.5	3.8
PA6-NSTEP*	368	420	11.6	8.6
PA6-NSTEP	334	407	13.3	6.8

[a] From derivative TG curves.
[b] At 463, 483 and 458 °C for PP, LLDPE and PA6, respectively.

Table 3
Thermogravimetric analyses in air.

Sample	$T_{onset10\%}$ [°C]	T_{max1} [a] [°C]	T_{max2} [a] [°C]	Residue at T_{max1} [b] [%]	Residue at T_{max2} [%]	Residue at 700 °C [%]
PP	278	323	480	38.5	1	1
PP-NS	268	325	434	39.0	1	1
PP-NSTEP	266	313	522	21.0	3.8	1
PP-NSTEP*	269	312	523	21.4	3.8	1
PP-NSAPP	270	327	540	48.7	12.4	5.0
LLDPE	359	406	537	52.5	2.0	1.4
LLDPE-NS	327	421	540	56.7	5.5	1.6
LLDPE-NSTEP	334	431	543	54.8	4.8	1.6
LLDPE-NSTEP*	335	431	546	55.0	5.0	1.7
LLDPE-NSAPP	378	434	596	81.0	10.2	6
PA6	403	450	556	45.6	3.0	0
PA6-NS	363	445	565	31.9	9.2	2.2
PA6-NSTEP*	359	421	585	21.2	10.7	2.6
PA6-NSTEP	332	416	583	23.3	13.2	2.7

[a] From derivative TG curves.
[b] At 323, 406 and 450 °C for PP, LLDPE and PA6, respectively.

than those of pure PP, PP-NS and PP-NSAPP; as a consequence, the corresponding residue is strongly reduced. Even though the second decomposition peak of PP is almost negligible (dTG in Fig. 3a, T_{max2}), all formulations turned out to shift this peak to higher temperatures. In general, the most interesting results have been achieved combining NS with APP since this complex showed a higher stability with respect to both the pure polymer and other TEP-based compounds (Fig. 3a).

Similarly to PP, the LLDPE degradation in air proceeds through two steps at 406 and 537 °C (Fig. 3b and Table 3). In this case, the nanosponges alone have been able to shift these maxima toward higher temperatures and form more residues with respect to the pure polymer. The joint effect between NS and TEP only slightly enhances the above performance, while much better results have been observed in the presence of APP. Indeed, the anticipation of the first degradation is not present anymore (see $T_{onset10\%}$ values) and the corresponding residues are much higher than those registered for LLDPE and LLDPE-NS.

As depicted in Fig. 3c, PA6-based formulations, irrespective of their composition, start to decompose at lower temperatures with respect to the pure polymer (see $T_{onset10\%}$ and T_{max1}, Table 3) and consequently the residues at T_{max1} decrease. In spite of this detrimental effect, both NS and their complexes are able to favour the carbonization of PA6 above 450 °C, shifting the second decomposition step (T_{max2}) toward higher temperatures and inducing the char formation, which is able to protect the polymer. As a consequence,

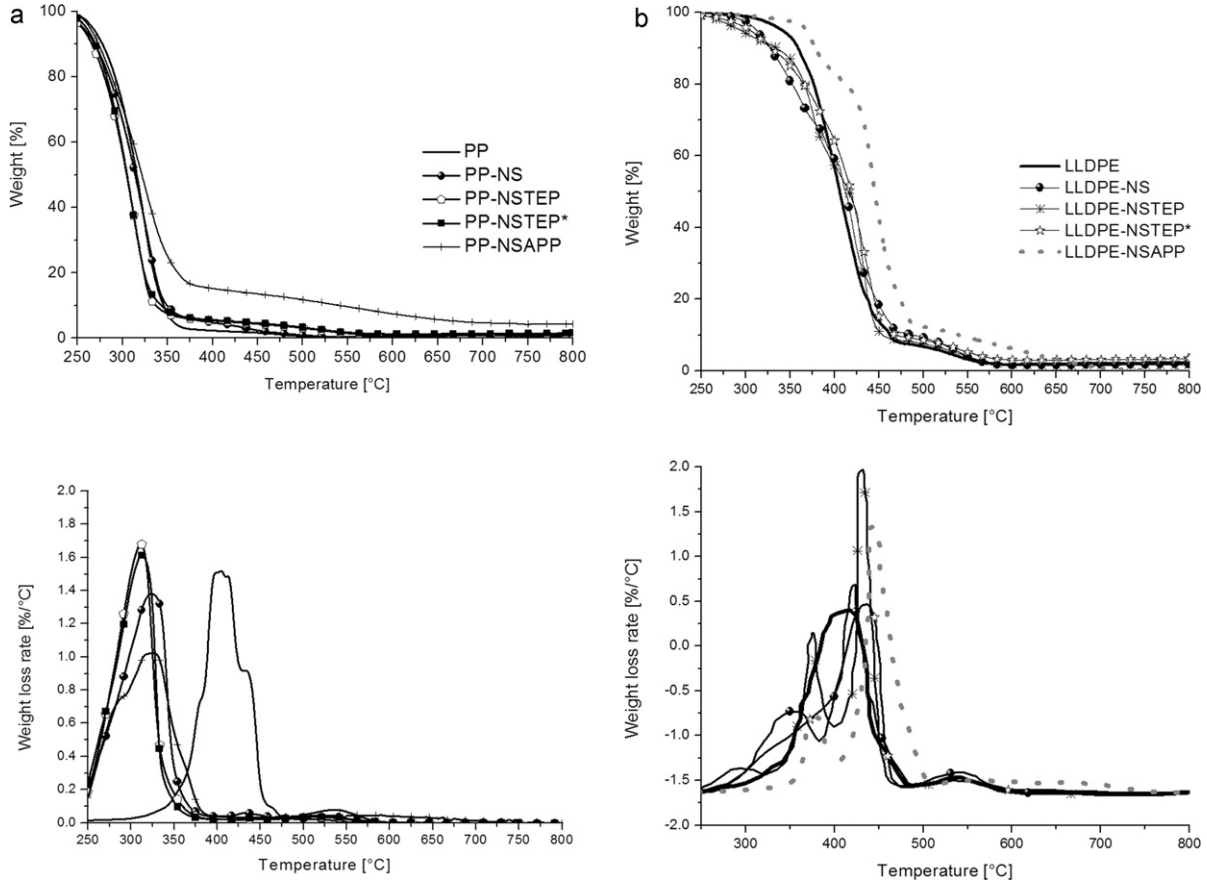

Fig. 3. TG and dTG curves of PP (a), LLDPE (b) and PA6 (c) systems in air.

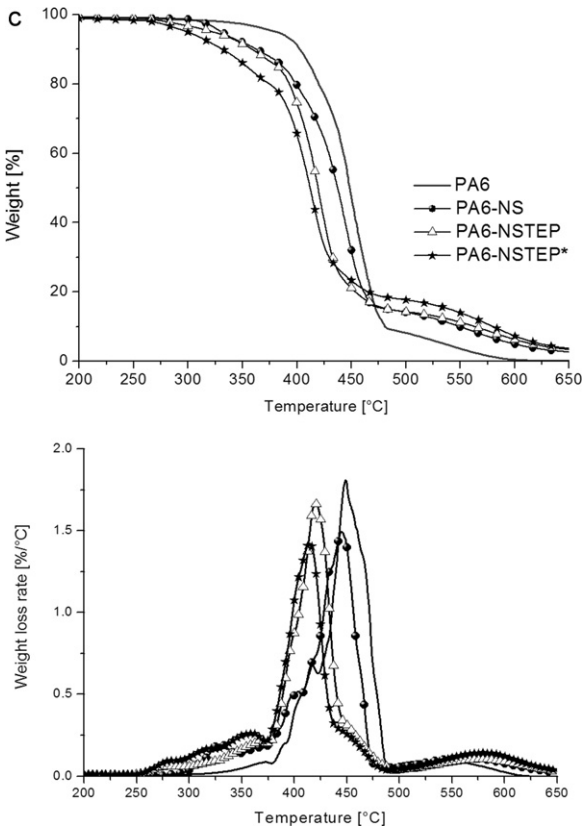

Fig. 3. (*continued*).

the final residue at 700 °C is still appreciable (Table 3, last column, last three lines).

The thermal properties of all the above samples in terms of melting and crystallization temperatures (T_m and T_c) and degree of crystallinity (X_c) have been evaluated by differential scanning calorimetry. Table 4 shows that the presence of both NS and NS complexes does not affect the T_m and T_c values of the polymers; on the contrary, as predictable, the X_c increases due to the presence of the flame retardants, which can act as crystallization seeds during the cooling down of the polymer.

3.2. Flame retardancy

The flame retardancy properties have been assessed by combustion and flammability tests.

Table 4
DSC data.

Sample	T_m [a] [°C]	T_c [b] [°C]	X_c [%]
PP	112	160	53
PP-NS	114	161	55
PP-NSTEP	119	161	55
PP-NSTEP*	117	160	60
PP-NSAPP	120	161	57
LLDPE	105	123	50
LLDPE-NS	107	122	56
LLDPE-NSTEP	107	123	53
LLDPE-NSTEP*	107	123	53
LLDPE-NSAPP	110	125	55
PA6	221	187	25
PA6-NS	221	189	29
PA6-NSTEP*	219	185	30
PA6-NSTEP	218	187	32

[a] From the 3rd scan.
[b] From the 2nd scan.

Cone calorimetry has been employed for investigating the effect of the proposed flame retardant systems on the behaviour of the different polymer matrices when subjected to a heat flow (namely, 35 kW/m^2). The collected data are listed in Table 5 while Fig. 4a–c shows the HRR values as functions of time for each formulation.

In general, it is possible to observe that the above flame retardants are responsible for a significant TTI anticipation, irrespective of the polymer type. This behaviour can be ascribed to two concurrent factors: first of all, as already discussed for data of thermogravimetric analyses, the hydroxyl functionalities of the nanosponges catalyse the decomposition of the three polymers in air. In addition, TEP and APP are typical flame retardants that act mainly in the condensed phase rather than the gas phase, so that they cannot play a significant role on the ignition of the combustion process upon heat irradiation (Horrocks, Davies, Alderson, & Kandola, 2007; Horrocks, 2008).

In detail, PP combustion slightly changes in the presence of the NS alone (Fig. 4a, full cycles); indeed, both THR and EHC, that represent the effective heat transfer from the polymer to the atmosphere, have been reduced (80 and 38.9 for PP-NS *vs.* 90 MJ/m^2 and 41.4 MJ/kg for PP, respectively – Table 5), as well as the combustion rate (pkHRR), which lowers from 1541 (pure PP) to 1462 kW/m^2 (PP-NS). The great advantage in the use of NS has been found in the smoke release: indeed, the smoke production rate, total smoke release and optical density (namely, SPR, TSR and SEA) of PP-NS turn out to be significantly lower than those determined for pure PP. When NS are coupled to phosphorus derivatives, only the two formulations containing 15 wt.% flame retardant (namely, PP-NSTEP* and PP-NSAPP) are capable to strongly decrease the pkHRR. Indeed, the all combustion mechanism for these latter formulations changes as clearly depicted by the HRR profiles (Fig. 4a). This behaviour can be also attributed to a foaming effect exerted by cyclodextrin nanosponges during their dehydration, due to phosphoric acid generation by TEP or APP. As a matter of fact, during the irradiation, a swollen structure is formed at the early stages of the thermal decomposition (first peak in the HRR curve) that subsequently collapses because of its incoherent feature. Thus, the production of volatile species is partially inhibited while the carbonization is favoured (second peak in the HRR curve).

However, these formulations are responsible for a significant increase of SPR. In addition, the formulation containing APP releases the highest smoke amount.

As far as LLDPE is considered (Fig. 4b), NS alone are not able to enhance the combustion resistance of the polymer. Indeed, all the parameters related to the heat transfer (i.e. THR, EHC and pkHRR) increase with respect to the pure polymer. Similarly to PP, the formulations containing 15 wt.% NS-phosphorus derivative complexes (i.e. LLDPE-NSTEP* and LLDPE-NSAPP) change the combustion mechanism (foaming effect of nanosponges), lowering the combustion rate but, at the same time, giving rise to higher amount of dark smokes.

Finally, NS do not impart any flame retardancy properties to PA6 (Fig. 4c), with the only exception of a significant THR decrease. When coupled to TEP, regardless of its content, nanosponges promote a substantial reduction of the heat of combustion and rate, as shown by the THR and pkHRR values collected in Table 5. At the highest TEP content (15 wt.%), a slight foaming effect is observed at the beginning of the combustion process. At the same time, SPR, TSR and SEA dramatically increase.

The flammability of the formulations under study has been tested measuring their resistance to an applied flame in terms of burning time and rate. The collected data are listed in Table 6.

First of all, NS turn out to be able to increase PP burning time and decrease its burning rate only when coupled to phosphorus derivatives: the best results refer to APP. However, a visual observation

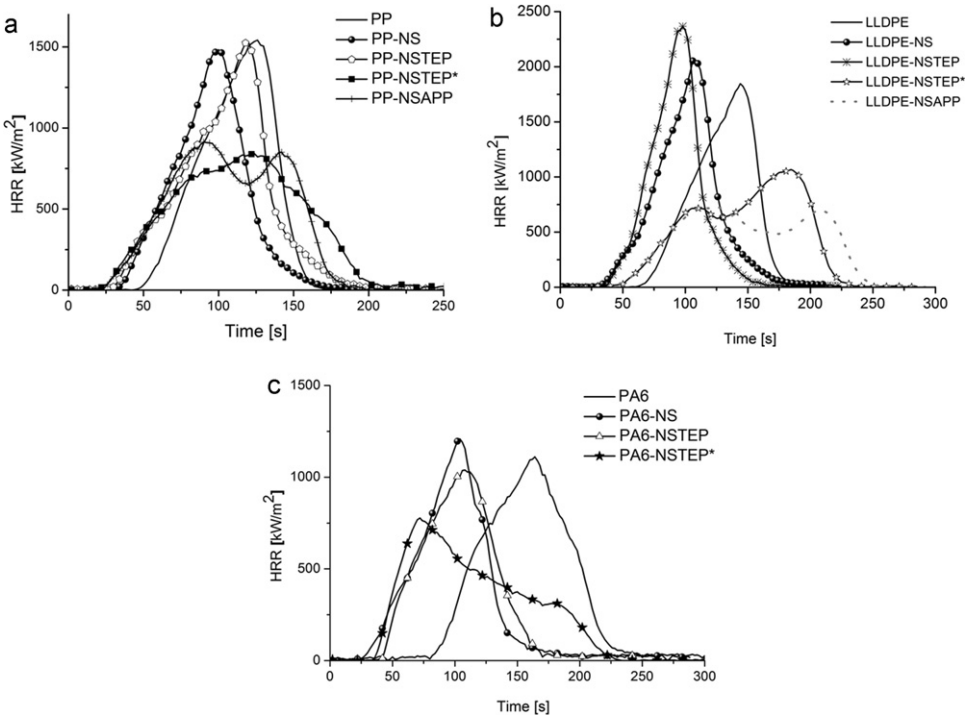

Fig. 4. HRR curves of PP (a), LLDPE (b) and PA6 (c) systems by cone calorimetry.

Table 5
Cone calorimetry data.

Sample	TTI [s]	pkHRR [kW/m^2]	THR [MJ/m^2]	EHC [MJ/kg]	SPR [m^2/s]	TSR [m^2/m^2]	SEA [m^2/kg]
PP	46	1541	90	41.4	0.066	1323	609
PP-NS	34	1462	80	38.9	0.037	1212	551
PP-NSTEP	30	1529	93	37.2	0.037	1182	457
PP-NSTEP*	26	839	90	40.2	0.059	1149	445
PP-NSAPP	24	910	89	40.0	0.050	1586	616
LLDPE	64	1823	103	40.3	0.056	1151	450
LLDPE-NS	34	2063	108	40.2	0.049	982	364
LLDPE-NSTEP	40	2366	105	43.1	0.063	1096	444
LLDPE-NSTEP*	50	1063	99	37.0	0.072	1205	584
LLDPE-NSAPP	46	728	98	35.8	0.060	1940	704
PA6	78	1111	90	29.1	0.030	398	134
PA6-NS	28	1196	76	27.6	0.035	351	128
PA6-NSTEP*	36	778	72	26.0	0.050	618	300
PA6-NSTEP	40	1030	73	26.8	0.046	755	280

Table 6
Flammability data.

Sample	Burning time [s]	Burning rate [mm/s]
PP	56	1.8
PP-NS	49	2.0
PP-NSTEP	71	1.4
PP-NSTEP*	101	1.0
PP-NSAPP	139	0.7
LLDPE	106	0.9
LLDPE-NS	62	0.6
LLDPE-NSTEP	54	0.5
LLDPE-NSTEP*	50	0.5
LLDPE-NSAPP	51	0.5
PA6	60	2.2
PA6-NS	25/89	1.1
PA6-NSTEP	25/125	0.8
PA6-NSTEP*	25/141	0.7

of the smokes released during the combustion confirms the results obtained by cone calorimetry: the APP-containing formulation develops the highest amount of dark smokes in comparison with both pure PP and PP-NS.

The only improvement for LLDPE systems refers to a reduction of the burning rate, irrespective of the formulation type or content.

PA6 shows the most interesting flammability results. NS alone are capable to protect the polymer from the flame: indeed, it has been necessary to apply the methane flame twice, in order to start the polymer burning (Table 6, last three entries of the second column). Furthermore, after the second flame application, the burning time strongly increases and the corresponding rate decreases. This result is in agreement with what has been already assessed for ethylene-vinyl-acetate copolymers (Alongi et al., 2010). This enhancement is further ameliorated when NS complexes are employed.

4. Conclusions

In the present paper, novel complexes of cyclodextrin nanosponges with triethylphosphate or ammonium polyphosphate molecules have been exploited for obtaining green flame retardants for PP, LLDPE and PA6. The polysaccharide-derived structure of the synthesized nanosponges turned out to play a key

role in the combustion behaviour and flammability of the aforementioned polymers, because of (i) the effective protection of the phosphorus derivatives exerted by NS during heating up of the polymers, which in turn determines the *in situ* generation of phosphoric acid at high temperatures; (ii) the NS significant contribution to the char formation; (iii) the intumescent features of NS, which act as foaming agents in the presence of high phosphorus contents.

Finally, combustion and flammability tests have shown the occurrence of a joint effect in between nanosponges and phosphorus derivatives.

Acknowledgement

The authors would like to thank Prof. Giovanni Camino for the fruitful discussions.

References

Alongi, J., Poskovic, M., Frache, A., & Trotta, F. (2010). Novel flame retardants containing cyclodextrin nanosponges and phosphorus compounds to enhance EVA combustion properties. *Polymer Degradation and Stability*, *95*, 2093–2100.

Bourbigot, S., & Duquesne, S. (2010). Intumescent-based fire retardants. In C. A. Wilkie, & A. B. Morgan (Eds.), *Fire retardancy of polymeric materials* (pp. 163–206). Boca Raton: CRC Press.

Bourbigot, S., Le Bras, M., Duquesne, S., & Rochery, M. (2004). Recent advances for intumescent polymers. *Macromolecular Materials and Engineering*, *289*, 499–511.

Duquesne, S., Magnet, S., Jama, C., & Delobel, R. (2005). Thermoplastic resins for thin film intumescent coatings towards a better understanding of their effect on intumescence efficiency. *Polymer Degradation and Stability*, *88*, 63–69.

Duquesne, S., Renault, N., Bardollet, P., Jama, C., Traisnel, M., & Delobel, R. (2009). Fire retardancy of polypropylene composites using intumescent coatings. In C. A. Wilkie, A. B. Morgan, & G. L. Nelson (Eds.), *Fire and polymers V, materials and concepts for fire retardancy* (pp. 192–204). USA: ACS Symposium Series 1013.

Enescu, D., Alongi, J., & Frache, A. (2012). Evaluation of nonconventional additives as fire retardants on polyamide 6,6: Phosphorus-based master batch, α-zirconium dihydrogen phosphate, and β-cyclodextrin based nanosponges. *Journal of Applied Polymer Science*, *123*, 3545–3555.

Feng, J. X., Su, S. P., & Zhu, J. (2011). An intumescent flame retardant system using β-cyclodextrin as a carbon source in polylactic acid (PLA). *Polymers for Advanced Technologies*, *22*, 1115–1122.

Hashidzume, A., Tomatsu, I., & Harada, A. (2006). Interaction of cyclodextrins with side chains of water soluble polymers: A simple model for biological molecular recognition and its utilization for stimuli-responsive systems. *Polymer*, *47*, 6011–6027.

Horrocks, A. R. (2008). Flame retardant/resistant textile coatings and laminates. In A. R. Horrocks, & D. Price (Eds.), *Advances in fire retardant materials* (pp. 159–187). Cambridge: CRC Press.

Horrocks, A. R., Davies, P., Alderson, A., & Kandola, B. K. (2007). The potential for volatile phosphorus-containing flame retardants in textile back-coatings. *Journal of Fire Sciences*, *25*, 523–540.

Huang, L., Allen, E., & Tonelli, A. E. (1999). Inclusion compounds formed between cyclodextrins and nylon 6. *Polymer*, *40*, 3211–3221.

Huang, L., Gerber, M., Lu, J., & Tonelli, A. E. (2001). Formation of a flame retardant-cyclodextrin inclusion compound and its application as a flame retardant for poly(ethylene terephthalate). *Polymer Degradation and Stability*, *71*, 279–284.

Le Bras, M., Bourbigot, S., Le Tallec, Y., & Laureyns, J. (1997). Synergy in intumescence – Application to β-cyclodextrin carbonisation agent in intumescent additives for fire retardant polyethylene formulations. *Polymer Degradation and Stability*, *56*, 11–21.

Le Bras, M., Camino, G., Bourbigot, S., & Delobel, R. (1998). *Fire retardancy of polymers – The use of intumescence*. Cambridge: The Royal Society of Chemistry.

Lorenzetti, A., Modesti, M., Besco, S., Hrelja, D., & Donadi, S. (2011). Influence of phosphorus valency on thermal behaviour of flame retarded polyurethane foams. *Polymer Degradation and Stability*, *96*, 1455–1461.

Morgan, A. B., & Wilkie, C. A. (2007). *Flame retardant polymer nanocomposites*. Hoboken: John Wiley & Sons.

Riva, A., Camino, G., Fomperiere, L., & Amigouet, P. (2003). *Polymer Degradation and Stability*, *82*, 341–346.

Tjong, S. C., & Bao, S. P. (2004). Preparation and nonisothermal crystallization behavior of polyamide 6/montmorillonite nanocomposites. *Journal of Polymer Science. Part B: Polymer Physics*, *42*, 2878–2891.

Wang, H., & Li, B. (2010). Synergistic effects of β-cyclodextrin containing silicone oligomer on intumescent flame retardant polypropylene system. *Polymers for Advanced Technologies*, *21*, 691–697.

Xie, W., Gao, Z., Pan, W. P., Hunter, D., Singh, A., & Vaia, R. (2001). Thermal degradation chemistry of alkyl quaternary ammonium montmorillonite. *Chemistry of Materials*, *13*, 2979–2990.